ACDIS

Research Report

Calibration and Extrapolation of a Simple Global Carbon Balance Model

Chenghao Ding
Department of Nuclear, Plasma, and Radiological Engineering
University of Illinois at Urbana-Champaign

Clifford E. Singer
Program in Arms Control & Domestic and International Security
University of Illinois at Urbana-Champaign

Research of the Program in Arms Control
& Domestic and International Security

University of Illinois at Urbana–Champaign

May 2022

The research for this publication is supported by the University of Illinois. It is produced by the Program in Arms Control & Domestic and International Security at the University of Illinois at Urbana-Champaign.

ACDIS Publication Series: The ACDIS *Occasional Paper* series is designed for circulating the scholarly analytical results of faculty, students, and visiting researchers associated with ACDIS. The ACDIS *Research Reports* series publishes technical reports and findings from security related research. The ACDIS *Commentary* series serves to inform U.S. and international policy decisions. The ACDIS *International Security Policy Brief* series contains previous works with a purpose similar to those in the *Commentary* series. ACDIS *Swords and Ploughshares* contains archives of a periodic journal of collected articles aimed at a general audience. For additional information and to download publications, visit the ACDIS home page at: http://acdis.illinois.edu/

Published 2022 by ACDIS//ACDIS DIN:1.2022

University of Illinois at Urbana–Champaign 359 Armory Building, 505 E. Armory Ave.
Champaign, IL 61820-6237

Series Editor: Jazmin Tejeda

Calibration and Extrapolation of a Simple Global Carbon Balance Model

CHENGHAO DING
Department of Nuclear, Plasma, and Radiological Engineering
University of Illinois at Urbana Champaign

CLIFFORD E. SINGER
csinger@illinois.edu
Program in Arms Control & Domestic and International Security
University of Illinois at Urbana Champaign

This report introduces a five-parameter model of the response of the atmospheric carbon dioxide concentration, $< CO_2 >$, to anthropogenic atmospheric carbon emissions. A fraction those emissions becomes promptly unavailable to the atmosphere. That fraction decreases as $< CO_2 >$ builds up. The remainder gradually equilibrates between the atmosphere and a surface and sea reservoir. The model parameters are calibrated against direct globally averaged measurements of $< CO_2 >$ from 1979–2019. Also used for calibration are published results of a *Gedankenexperiment* starting with preindustrial $< CO_2 >$, increasing it exponentially at a rate of 1%/year, and then decaying after anthropogenic carbon emissions abruptly cease. Historical emissions are fit with a sum of a logistic function and two functions that are proportional to derivatives of logistic functions. Extrapolations of $< CO_2 >$ are shown with those fits and four global "Green Deal" emissions futures.

1. Motivation and Calibration

The present approach was motivated by a need for readily understandable and rapidly computable $< CO_2 >$ extrapolations for use in human participant simulations of the economic impacts of climate change policy options [1]. Previously, a data-calibrated model used for this purpose accounted only for a decrease in solubility of CO_2 with increasing ocean water acidity [2]. That model did not allow for a decrease in $< CO_2 >$ following a substantial reduction or elimination of future anthropogenic carbon emissions. (Herein, the content of carbon in anthropogenic emissions of CO_2 is referred to simply as emissions. Also, the references here to atmospheric carbon refer only to carbon in CO_2 and include neither comparatively very small amounts of carbon in other gases nor carbon in non-gaseous form.) The present approach reproduces a least squares fit to a *Gedankenexperiment* example from a Zero Emissions Commitment Model Inter-comparison Project (ZECMIP) that shows a substantial $< CO_2 >$ reduction after abrupt termination of emissions [3, 4]. The equations used here are

$$a' = f_e e_c - s' \tag{1.1}$$

$$s' = \nu(r_{sa} a - s) \tag{1.2}$$

Here e_c is emissions in TtonneC/yr and a and s are respectively the TtonneC carbon content of the atmosphere and of a reservoir in the earth's surface and oceans. Annual rates of change of these quantities are a' and s'. In the absence of emissions, and also after an approach to their eventual elimination, the values of a and s respectively start with and eventually approach equilibria with a constant ratio $r_{sa} = s/a$. The fraction f_e of emissions that partition between a and s is

$$f_e = 1 + (f_m - 1)e^{-(a-a_0)/a_3} \tag{1.3}$$

where a_0 is the year 1750 atmospheric carbon content in CO_2. The remaining fraction $(1 - f_e)$ is assumed to remain sequestered away from exchange back into the atmosphere on time scales of interest here. For graphical purposes, the computed value of a is divided by $c_1 = 0.002124$ TtonneC/ppm [5] to convert to $< CO_2 >$ in parts per million by volume. The values of c_1, ν, r_{sa}, f_m, and a_3 are listed in Table 1, along with other constants to be discussed below. Values

of parameters referring to atmospheric carbon content are also listed as $< CO_2 >$ equivalents in Table 1.

Table 1. Carbon Balance Constants

Symbol	Value	Units	ppm	Description
a_0	0.592	TtonneC	287.7	atmospheric carbon in CO_2 in 1750
f_m	0.581	1		minimum prompt sequestration escape fraction
a_3	0.524	TtonneC	246.8	constant affecting increase in sequestration escape
ν	0.01285	1/yr		a and s equilibration rate
r_{sa}	1.53311	1		s/a ratio in equilibrium
c_1	0.002124	TtonneC/ppm		convert $< CO_2 >$ to atmospheric TtonneC
μ	0.01	1/yr		*Gedankenexperiment* $< CO_2 >$ growth rate
ρ	0.03256	1/yr		*Gedankenexperiment* $< CO_2 >$ decay rate
a_1	1.096	TtonneC	516.2	*Gedankenexperiment* maximum atmospheric carbon
a_2	0.877	TtonneC	412.9	*Gedankenexperiment* long-term atmospheric carbon

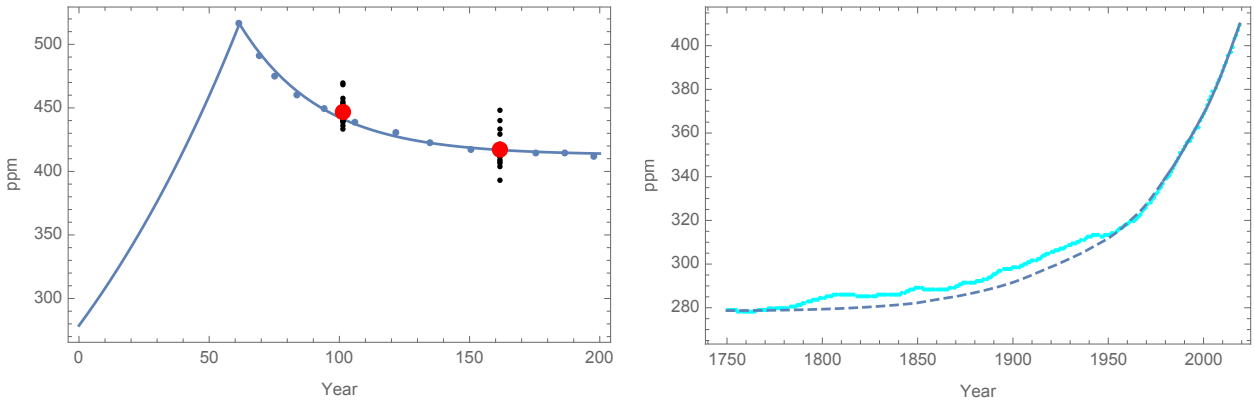

Figure 1. (a) Evolution of $< CO_2 >$ with exponential growth at 1%/yr followed by decline after an abrupt halt to carbon emissions, compared to results from a GFDL-ESM calculation (dots near the curve) and 18 ZECIMP project cases (small dots) and their averages (large dots). (b) Comparison of $< CO_2 >$ data to solutions from equations (1.1) and (1.2) using Table 1 values of r_{sa}, ν, a_3, and f_m, along with simulation results for earlier years (dashed curve) and corresponding years' data not used for parameter estimation.

Parameters in the escape from prompt sequestration fraction function, f_e, were estimated from a least squares fit to global average direct measurements [6] of $< CO_2 >$. Only $< CO_2 >$ global averages based on the direct atmospheric measurements for 1979–2019 were used for this calibration; but Figure 1b also compares $< CO_2 >$ from ice cores [7] to solution of the above global carbon balance equations. Before 1750, $< CO_2 >$ is approximated as constant, as are emissions of 0.000077 TtonneC/yr listed in Table 1 dominated by land use changes, that rate of emissions is subtracted from the total emissions when computing the evolution of $< CO_2 >$ shown in Fig. 1b and the extrapolation results shown in Fig. 3b. Rationale and methods used for estimating the values of f_m and a_3 listed in Table 1 and used in equation (31.3) are described in Appendix A below.

Table 2. Carbon Emissions Constants

Type, with Units in TtonneC yr^{-1}	b_0	b_1	b_2 (Julian Year)	b_3 (yrs)
Industrial $b_0 + b_1 u$	-0.000002	0.015285	2002.57	27.82
Land Use Early $b_0 + b_1 u(1-u)$	-0.000075	0.005940	1950.98	46.20
Land Use Late $b_1 u(1-u)$	0	0.002967	2021.63	8.91

2. No New Policy Emissions Extrapolations ± Fluid Fossil Fuel Depletion Effect

Figure 2a compares the emissions function fit using Table 2 parameters to the input emissions data [8] over the time range 1850–2019, without the small constants b_0 included in the fit. Figure 2b shows that function fit extrapolated to cover the range of years 1750–2120, with the contants b_0 included so what is plotted is the increase over the year 1750. The upper curve in Figure 2b has emissions equal to $e_{\rm ind} + e_{\rm land}$, where $e_{\rm ind}$ is is from the first line in Table 2 and $e_{\rm land}$ is from the sum of early and late land use formulas in Table 2.

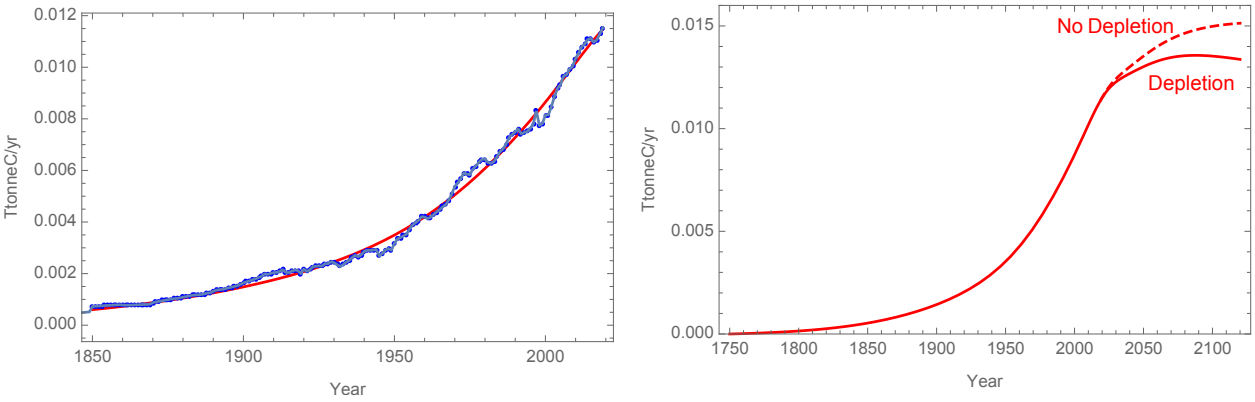

Figure 2. (a) Comparison of anthropogenic carbon emissions data and functional fit. (b) Functional fit to data shown in Figure 2a, extrapolated to 1750 and 2120 without (upper curve) and with (lower curve) fluid fossil fuel depletion effect included.

The lower curve in Figure 2b includes a correction for the effect of depletion of more readily extractable resources of fluid fossil fuels (i.e. of natural gas and oil). The corresponding formula for extrapolated emissions is

$$e_c = f_c e_{\rm ind} + (1 - f_c) f_d e_{\rm ind} + e_{\rm land} \tag{2.1}$$

where

$$f_d = \left(1 + \frac{1 + b_d {\rm Max}[U, U_{2019}]}{1 + b_d U_{2019}}\right)^{\beta_f} \tag{2.2}$$

The formula for cumulative sum of industrial atmospheric carbon emissions is

$$U = -b_1 b_2 + b_1 b_3 \ln[e^{b_2/b_3} + e^{t/b_3}] + b_0 (t - 1750) \tag{2.3}$$

where b_0, b_1, b_2, and b_3 are from the first row of numbers in Table 2. The value of $U_{2019} = 0.44$ TtonnneC listed in Table 3 is the cumulative global industrial atmospheric carbon emissions U from 1750 to 2019. Extrapolated carbon emissions from industrial coal use in equation (2.1) are taken to continue their recent 1965-2019 fraction f_c of what total extrapolated industrial emissions would be in the absence of fossil fuel depletion effects. The rationale for this approach is noted in Appendix A, as is the data used for estimating of the value $f_c = 0.41$ listed in Table 3.

Including the expression $\mathrm{Max}[U, U_{2019}]$ in the equation for the fluid fossil fuel resource depletion factor f_d is a shorthand way of expressing that this depletion effect applies only to extrapolation of anthropogenic atmospheric carbon emissions after 2019. The idea behind this approach is that historically a globally commercially competitive market in fossil fuels had yet to evolve, and technological advances had helped to balance the cost escalation effect of resource depletion. However, impacts of technological advances in resource extraction have physical limits. Also, depletion of regional geologic resources is assumed to eventually drive extraction costs higher than transportation costs, leading to evolution of global markets for both natural gas and oil. Any model of the long-term evolution of resource depletion effects on the future of carbon emissions is necessarily very approximate. Here, this effect accounts for a 5% reduction in extrapolated emissions by 2060, and it allows for continued growth in extrapolated emissions up to 2088. Inclusion of the resource depletion effect is in practice not particularly important, but conceptually it recognizes that depletion of geologically limited competitive fluid fossil fuel resources may eventually constrain the growth of their use that helped drive a rapid rise in global atmospheric carbon emissions after World War II.

Table 3. Carbon Balance Constants

Symbol	pp4	Value	Units	Description
g_c	0.32	1		coal fraction of 1965–2019 fossil energy use
f_c	0.41	1		coal fraction of 1965–2019 carbon emissions
b_d	0.68	1/TtonneC		fluid fossil fuel depletion effect coefficient
β_f	-0.35	1		fluid fossil fuel demand elasticity exponent
U_{2019}	0.44	TtonneC		cumulative industrial emissions through 2019

Table 3 lists coal fractions of energy production and carbon emissions, g_c and g_f, the extraction cost escalation coefficient, b_d, and the price elasticity of demand, β_f. Methods for estimating these constants and those in the above expression for e_c are described in Appendix A.

3. Green Deal Examples

Figure 3 shows the evolution $< CO_2 >$ resulting from different sets of globally uniform policy choices. Each case has extrapolated emissions from equations (1.2) and (1.3)multiplied by the factors shown in Figures 3a. For the Hard, Reference, and Soft cases in Figure 3, zero anthropogenic carbon emission is approached asymptotically along different pathways. For each policy choice, extrapolated emissions given by equations (2.1)–(2.3) are multiplied by $(1 - g_1 + g_1 f_p/f_{p0})$. Results are also shown in Figure 3 with the same Reference curve parameters but with $g_1 = 1/3$ and $2/3$.

$$f_p = (f_{45} - f_{23})y + g_3(1 + f_{23}) \ln[e_{y3} + e_{23}] - g_5(1 + f_{45}) \ln[e_{y5} + e_{45}] \tag{3.1}$$

with $e_{23} = e^{g_2/g_3}$, $e_{45} = e^{g_4/g_5}$, $e_{y3} = e^{y/g_3}$, $e_{y5} = e^{y/g_5}$, $f_{23} = 1/e_{23}$, $f_{45} = 1/e_{45}$, $y = t - 2019$, and f_{p0} is the value of f_p evaluated for $y = 0$. While this function looks complicated, the description in the next paragraph of the function of the constants $g_1 \ldots g_5$ clarifies how they allow for a readily understandable and flexible choice of policy options to explore.

The conceptual starting point for all of the cases shown here is a straight line decrease of the extrapolated emissions multiplier. Modifying that are (i) a slower start after 2019 and (ii) avoidance of an abrupt transition towards zero emissions when approaching the zero emissions point of a linear emissions multiplier. The idea behind the smoother final transition to zero emissions is that that phase is the most expensive part of the emissions reductions process to implement, and thus may be likely to be taken more slowly. The idea behind the slower start of a global cooperation is that

it would take time to arrange widespread cooperation. Emissions reductions multipliers are applied starting in 2019. No attempt is made to model the very small impact of possibly very transient emissions reductions that occurred in 2020 [9]. The effects of these minor transients on the overall evolution of $< CO_2 >$ is taken to be negligible compared to that of the policy options examined here.

The parameter g_1 is the fraction of global carbon emissions implementing a Green Deal policy. The annual rate of change of the function f_p is $s_{23} - s_{45}$ where s_{23} and s_{45} are smoothed step functions. Here $s_{45} = u_{45} - e^{-(g_4/g_5}(1 - u_{45})$, where $u_{45} = 1/(1 + e^{-(y-g_4)/g_5})$ is a unit logistic function. Thus, an emissions reductions policy is half way to start of implementation after g_4 years on a path with a startup timescale of g_5 years. Similarly, $s_{23} = u_{23} - e^{-g_2/g_3}(1 - u_{23})$, where $u_{23} = 1/(1 + e^{-(y-g_2)/g_3})$. An emissions reduction policy is gradually terminated on a timescale of g_3 years with the termination phase being half way to completion g_2 years after 2019.

Table 4 lists the values of parameters used for different policy choice cases. Figures 3a–4b all show results for a Reference "Full Green Deal" cases with $g_1 = 1$. The Reference case has a startup delay of $g_4 = 4$ years and an additional transition time to a nearly linear decline in the emissions multiplier of $g_5 = 4$ years. The target time for continuation of that nearly linear emissions multiplier decline is $g_2 = 30$ years, and the timescale for pursuing the final approach towards zero emissions is $g_3 = 8$ years. The Hard case results shown in Figure 3b assume an abrupt transition to final approach to zero global emissions, on a $g_3 = 2$ year timescale.

Table 4. $g_2 \ldots g_5$ in Years

Case	g_2	g_3	g_4	g_5
Reference	30	8	4	4
Hard	30	2	4	4
Soft	30	24	4	4
Early	20	8	4	4
Late	40	8	4	4
Prompt	30	8	2	2
Slow	30	8	8	8

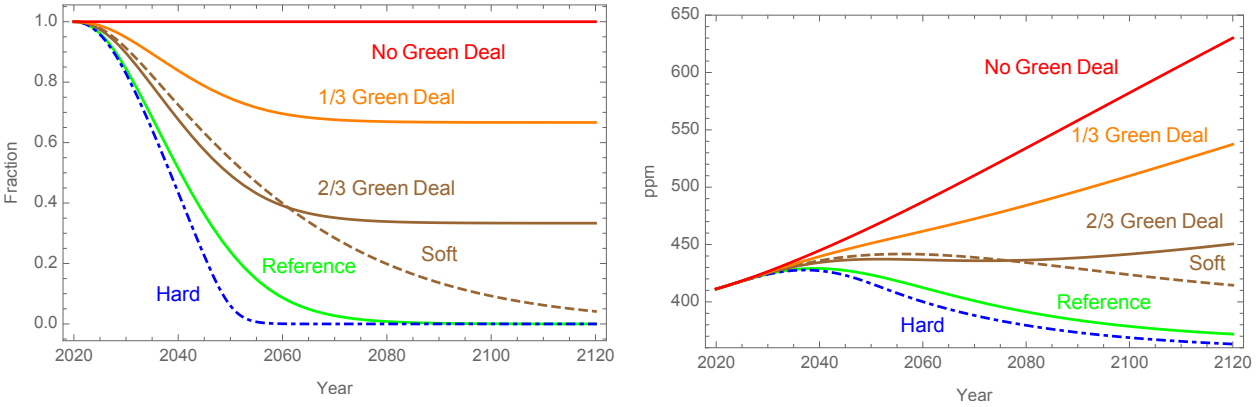

Figure 3. a) Carbon emission multipliers and (b) $< CO_2 >$ with first three rows of numbers in Table 4 and either $g_1 = 1$ or the indicated Green Deal fraction.

Compared to the artificial *Gedankenexperiment* result in Figure 1a, the Reference case does not result is as much reduction in $< CO_2 >$ below its maximum value. However, this case does allow

for a reduction in $< CO_2 >$ below its year 2019 and maximum year values without the need for as abrupt a final transition to zero emissions as in the Hard case. This type of flexibility may be of interest in policy negotiation simulations.

The Soft case in Figure 3a assumes global cooperation on a much more gradual transition towards zero emissions. The result for $< CO_2 >$ in Figure 3b for the current century is nearly the same as for 2/3 global cooperation on the Reference case timescales. Without either the Soft or 2/3 Green Deal levels of global cooperation, $< CO_2 >$ continues to increase through the current century and beyond.

Figures 4a and 4b compare emissions multipliers for the reference Green Deal case plotted in Figure 3a to examples also computed with $g_1 = 1$ but using the last four rows of numbers in Table 4. Figure 4a illustrates how the time scale the rate of final approach to zero global emissions can be varied. Figure 4b illustrates how the time it takes to start substantive implementation of policies to limit emissions can be varied. Since the evolution of $< CO_2 >$ is for the cases shown in Figures 4a and 4b is similar to that for the Reference case, the point of including these figures is just to illustrate how flexibility in specifying different emissions policies is built into the single formula in equation 3.1.

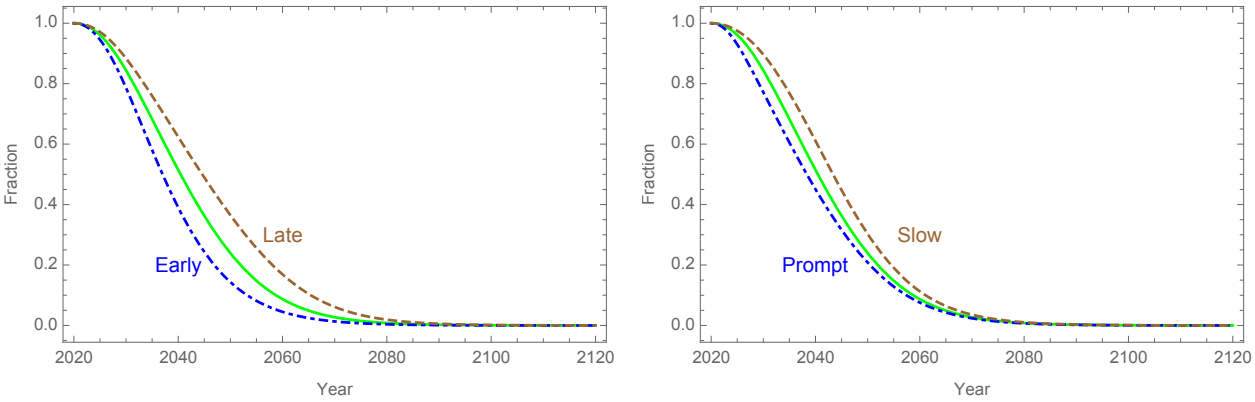

Fig. 4. (a) Carbon emission multipliers with associated parameters in Table 4 and the emission multiplier formula in equation (4.1) for (a) Early and Late cases and (b) Prompt and Slow cases.

4. Summary

The results shown here illustrate how a simple but systematically calibrated global carbon balance model can be used to extrapolate the evolution of $< CO_2 >$ for a variety of policies concerning anthropogenic carbon emissions. The key point is that there are various options for keeping $< CO_2 >$ well below doubling of the preindustrial level and limiting it to less than 10% higher than the year 2019 level for 100 years. This is *provided* that the breadth of cooperation on emissions limitations illustrated by the Soft or 2/3 Green Deal cases shown in Figures 3a and 3b could be achieved.

Appendix A. Calibration and Extrapolation Methods

A.1. **Calibration.** The initial condition for integrating the global carbon balance equations starts from an assumed equilibrium with a value $s_0 = r_{as} a_0$ in 1750. For integrating the carbon balance equations to get the curve shown in Figure 1b, a linear interpolation of annual estimates of global carbon emissions was used. For 1850–2019, those estimates were the data points shown in Figure 2a. Those numbers are the sums of industrial emissions (less recarbonization due to atmospheric exposure of cement [10]) plus land use emissions [5, 8], plus the sum of the (negative) values

of b_0 in Table 2. From 1750–1849, those annual emissions estimates were from the evaluations of the emission fitting function using the fitting parameters listed in Table 2.

Estimates of the parameters f_m and a_3 listed in Table 1 and used in equation (3.1) are from minimizing the sum of the squares of the differences between the points and curve values for the 1979–2019 portion of Figure 2.1b. Using only the global average estimates of $< CO_2 >$ based on direct atmospheric measurement avoids mixing data sources with different temporal resolution and with periods of large and smaller average growth compared to a steady growth trend. The approach used here is taken to be suitable for a goal of extrapolating more recent historical trends rather than analyzing in detail the uncertainties in earlier historical data estimates and methods for fitting that data.

A.2. **Fluid Fossil Fuel Depletion Effect on Extrapolation.** The extrapolation of a historically calibrated fit to emissions shown as the dashed curve in Figure 2b increases monotonically forever, an impossible result given limits on economically competitive extraction of finite fossil fuel resources. For perspective on this question, Table 5 lists parameters for linear fits to the cost of extracting geological resources [11] of natural gas, oil, and coal as a function of cumulative total resource depletion. Market prices include transportation and other costs approximated here to be equal to the average of the intercepts in inflation adjusted dollars (USD2020) per GJ of combustion energy listed in Table 5. The average U.S. crude oil import price for 1990–2019 was 8.9 USD2020 per GJ ($54/barrel) [12]. The formula used here back-extrapolated to 2005 gives 9.6 USD/GJ. Given the volatility of oil prices, a simple factor of two was used for the ratio of prices due to fixed costs and the average of the zero resource depletion intercept for oil and natural gas. This despite that a measure of the average international price of natural gas over the same period at 6.6 USD/GJ ($7.0 per million British Thermal Units) is lower than the per unit energy oil price. A global market price for natural gas is difficult to discern in view of what remains a regionally fragmented market and is thus not considered to be definitive enough to prompt revision of the simple approach used here. The slopes listed in Table 5 for these fits are in units of USD2020/GJ per ZJ of cumulative global depletion for each fossil fuel resource. The slope listed in Table 5 for coal is so much smaller than for natural gas and oil that the impact of resource depletion on price and use of coal is neglected here.

With rates of future energy from natural gas and oil approximated as being equal in the very approximate analysis here, the average cost P of natural gas and oil is $P = b_{\rm ff} + m_{\rm ff}Z$, where $b_{\rm ff} = b_{\rm gas} + b_{\rm oil}$ from Table 5 and $m_{\rm ff} = (m_{\rm gas} + m_{\rm oil})/2$. (The value of $b_{\rm ff}$ is twice the average of the natural gas and oil intercepts, for reasons noted in the previous paragraph.) Here $Z = g_f Z_{\rm total}$ is approximated as equal cumulative energy from depletion of natural gas, and of oil, and $Z_{\rm total}$ is the cumulative total global energy from fossil fuels. Since the resource depletion effect is small, for simplicity the value of $g_f = (1 - g_c)/2 = 0.34$ for the fractions each of extrapolated energy use from natural gas and oil is used in the equations in the next paragraph. Here $g_c = 0.32$ is the nearly constant fraction (with a standard deviation of 0.026) of global fossil fuel energy from coal for 1965–2019 [14].

Using the carbon emission intensities of fossil fuel combustion constants r listed [15] in Table 5 gives $U_c = (c_{\rm gas}g_f + c_{\rm oil}g_f + c_{\rm coal}g_c)Z_{\rm total}$ with $Z_{\rm total} = Zg_f$. Using this to eliminate Z in favor of U_c in $P = b_{\rm ff} + m_{\rm ff}Z$ gives $P = b_{\rm ff}(1 + b_d U_c)$ with the value of b_d listed above in Table 3. The formula f_c=$r_3 g_c/(r_3 g_c + (r_1 + r_2)(1 - g_c)/2)$ gives the value $f_c = 0.41$ listed in Table 3 and used in equation (2.1). Here g_c is the 1965–2019 average coal fraction of fossil energy combustion energy listed in Table 3. The fraction f_c of carbon emissions from coal is larger than the fraction g_c of fossil fuel energy from coal because coal is a more carbon-intensive energy sourse than fluid fossil fuels.

Table 5. Fossil Fuel Depletion Constants

Symbol	Units	Natural Gas	Oil	Coal
Fuel type		1	2	3
b	USD2020/GJ	3.1167	4.5591	3.0320
m	(USD2020/GJ)/ZJ	0.2816	0.3018	0.0354
r	TtonneC/ZJ	0.0137	0.0193	0.0247

The above-mentioned price elasticity of demand of β_f= -0.35 is taken here to correspond to market price rather than extraction cost. The value of β_f used here comes from an analysis of Mexico [16], a middle per capita income country with a low coal fraction of energy use. The implicit assumption here is that consumption of fluid fossil fuels will eventually respond to evolution of a global market price, around which oscillations occur, because incremental cost changes associated with resource depletion effects will come to dominate over fuel transport costs and other factors that set a minimum global average market price. Taking the ratio of the modeled market price to its 2019 value to the β_f power gave the formula and parameter values described above for the impact of fluid fossil fuel resource depletion on extrapolated emissions. The complication of removing a correction for the portion of industrial emissions from concrete [8, 10], is also avoided, since accounting for that only had about a 1% effect on the estimated parameter values.

For coal, the corresponding value of the coefficient m in Table 5 is about 1/8 of that for fluid fossil fuels, so no resource depletion effect is included in the contribution to extrapolated carbon emissions from coal. Increases in use of coal are assumed to be limited by regional pollution concerns even if resource depletion increases the cost of fluid fossil fuels, so for simplicity no effect on coal use of elasticity of substitution between coal and fluid fossils fuels is included. For cumulative emissions compatible with the cases above in Figures 3 and 4, the resource depletion effect has little impact on the results. However, the resource depletion effect is more significant for examples that allow for larger cumulative emissions while limiting global average temperature through solar radiation management, e.g. via stratospheric sulfur injection. Preparation for such additional applications of the present model is one reason that this effect is included. Also, isubsequent work examining the impact of different regional policies on carbon emissions limits price elasticity of demand is planned. That is because one or more regions limiting fluid fossil fuel use would limit resource depletion and should thus limit global market price increases. Accounting for price elasticity of demand for fluid fossil fuels will avoid implicitly assuming that a reduction by emissions from one region will lead to an equal reduction in global emissions.

References

[1] Singer, C., and L. Matchett, 2016. Climate action gaming experiment: Methods and example results, *Challenges* **6**, 202-228, doi 10.3390/challe6060602.

[2] Milligan, T. 2012. Development of an econo-energy model and an introduction to a carbon and climate model for use in nuclear energy analysis. University of Illinois at Urbana-Champaign Master's Thesis, http://hdl.handle.net/2142/31168.

[3] MacDougall, A. H., T. L. Frölicher, C. D. Jones, J. Rogelj, H. D. Matthews, K. Zickfeld, V. K. Arora, N. J. Barrett, V. Brovkin, F. A. Burger, M. Eby, A.V. Eliseev, T. Hajima, P. B. Holden, A. Jeltsch-Thömmes, C. Koven, N. Mengis, L. Menviel, M. Michou, I. I. Mokhov. A. Oka, J. Schwinger, R. Séférian, G. Shaffer, A. Sokolov, K. Tachiiri, J. Tjiputra, A. Wiltshire, and T. Ziehn. 2020. Is there warming in the pipeline? A multi-model analysis of the Zero Emissions Commitment from CO_2. *Biogeosciences*, **17**, 2987–3016, https://doi.org/10.5194/bg-17-2987-2020/.

[4] Jones, C. D., T. L. Frölicher, C. Koven, A. H. Macdougall, H. D. Matthews, K. Zickfeld, J. Rogelj, K. B. Tokarska, N. P. Gillett, T. Ilyina, M. Meinshausen, N, Mengis, R. Séférian, M. Eby, and F. A. Burger. 2019. The Zero Emissions Commitment Model Intercomparison Project (ZECMIP) contribution to C4MIP: quantifying

committed climate changes following zero carbon emissions. *Geoscientific Model Development* **12**, no. 10, 4375-4385. https://doi.org/10.5194/gmd-12-4375-2019.

[5] Friedlingstein, P., M. O'Sullivan, M. W. Jones, R. M. Andrew, J. Hauck, A. Olsen, G. P. Peters, W. Peters, J. Pongratz, S. Sitch, C. Le Quéré, J. G. Canadell, P. Ciais, R. B. Jackson, S. Alin, L. E. O. C. Aragão, A. Arneth, V. Arora, N. R. Bates, M. Becker, A. Benoit-Cattin, H. C. Bittig, L. Bopp, S. Bultan, N. Chandra, F. Chevallier, L. P. Chini, W. Evans, L. Florentie, P. M. Forster, T. Gasser, M.Gehlen, D. Gilfillan, T. Gkritzalis, L. Gregor, N. Gruber, I. Harris, K. Hartung, V. Haverd, R. A. Houghton, T. Ilyina, A. K. Jain, E. Joetzjer, K. Kadono, E. Kato, V. Kitidis, J. I. Korsbakken, P. Landschützer, N. Lefévre, A. Lenton, S. Lienert, Z. Liu, D. Lombardozzi, G. Marland, N. Metzl, D. R. Munro, J. E. M. S. Nabel, S. Nakaoka, Y. Niwa, K. O'Brien, T. Ono, P. I. Palmer, D. Pierrot, B. Poulter, L. Resplandy, E. Robertson, C. Rödenbeck, J. Schwinger, R. Séférian, I. Skjelvan, A. P. Smith, A. J. Sutton, T. Tanhua, P. P. Tans, H. Tian, B. Tilbrook, G. van der Werf, N. Vuichard, A. P. Walker, R. Wanninkhof, A. J. Watson, D. Willis, A. J. Wiltshire, W. Yuan, X. Yue, and S. Zaehle. 2020. Global Carbon Balance 2020. *Earth System Science Data*
pmb12, 3269–3340, https://doi.org/10.5194/essd-12-3269-2020.

[6] Butler, J. H., and S. A. Montzka. 2017. The NOAA annual greenhouse gas index (AGGI), https://www.esrl.noaa.gov/gmd/aggi/aggi.html, accessed 6 December 2020.

[7] Etheridge, D. et al. 2010. Law Dome Ice Core 2000-Year CO2, CH4, and N2O Data. IGBP PAGES/World Data Center for Paleoclimatology Data Contribution Series # 2010-070. NOAA/NCDC Paleoclimatology Program, Boulder CO, USA, ftp://ftp.ncdc.noaa.gov/pub/data/paleo/icecore/antarctica/law/law2006.txt, and references therein, including Etheridge, D. M., L. P. Steele, R. L. Langenfelds, R. J. Francey, J.-M. Barnola, and V. I. Morgan. 1996. Natural and anthropogenic changes in atmospheric CO2 over the last 1000 years from air in Antarctic ice and firn, *Journal of Geophysical Research*, **101**, 4115–4128, https://doi.org/10.1029/95JD03410.

[8] Global Carbon Budget 2020 (Version 1.0) [Data set]. Supplemental Data. Global Carbon Project. 2020. https://doi.org/10.18160/gcp-2020. (https://www.icos-cp.eu/science-and-impact/global-carbon-budget/2020, accessed July 1, 2021).

[9] Global Carbon Budget. 2021. Data supplement to the global carbon budget 2021. https://www.icos-cp.eu/science-and-impact/global-carbon-budget/2021, accessed December 6, 2021.

[10] Andrew, R. M. 2019. Global CO_2 emissions from cement production, 1928–2018. *Earth System Science Data* **11**, 1675-1710, https://essd.copernicus.org/articles/11/1675/2019/

[11] Rogner, H-H., 1997. An assessment of world hydrocarbon resources, *Annual Review of Energy and the Environment* **22**, 217-262, https://www.annualreviews.org/doi/abs/10.1146/annurev.energy.22.1.217.

[12] U.S. Energy Information Agency. 2021. F.O.B. Costs of imported crude oil by area, December 1, https://www.eia.gov/dnav/pet/pet_pri_imc1_k_m.htm, accessed December 7, 2021.

[13] Federal Reserve Economic Data. 2021. Global price of natural gas, EU, November 24, https://fred.stlouisfed.org/series/PNGASEUUSDM#, accessed December 7, 2021.

[14] BP. 2021. BP Statistical Review of World Energy 2021. https://www.bp.com/en/global/corporate/energy-economics/statistical-review-of-world-energy.html, accessed January 10, 2020.

[15] U.S. Environmental Protection Agency. 2019. User's guide for estimating direct carbon dioxide emissions from fossil fuel combustion using the State Inventory Tool. November. https://www.epa.gov/sites/default/files/2017-12/documents/co2, from_fossil_fuels_users_guide.pdf, accessed August 10, 2021.

[16] Huntington, H. G., J. J. Barrios, and V. Arora. 2017. Review of key international demand elasticities for industrializing economies. Energy Information Agency Working Paper Series, December. https://www.eia.gov/workingpapers/pdf/key_international_demand_elasticities.pdf, accessed August 10, 2021.